10.17951/aa.2019.74.2.89-100

ANNALES
UNIVERSITATIS MARIAE CURIE-SKŁODOWSKA
LUBLIN – POLONIA
VOL. LXXIV, 2 SECTIO AA 2019

Activity and stability of cobalt-manganese catalysts in the process of methane flameless combustion

Marek Rotko[a*], Vladyslav Redko[b] and Witold Zawadzki[a]

[a] *Maria Curie-Sklodowska University, Faculty of Chemistry,*
Institute of Chemical Sciences, Department of Chemical Technology,
3 Maria Curie-Sklodowska Square, 20-031 Lublin, Poland
[b] *Medical University of Gdańsk, Faculty of Health Sciences with Subfaculty*
of Nursing with Institute of Maritime and Tropical Medicine,
Department of Environmental Toxicology, Dębowa 23 A, 80-204, Gdańsk, Poland
[*] *e-mail: marekrotko@poczta.umcs.lublin.pl*

Oxide cobalt-manganese catalysts with different contents of cobalt and manganese, as well as pure cobalt and manganese catalysts have been tested in the process of methane flameless combustion (complete catalytic oxidation). The X-ray diffraction and X-ray photoelectron spectroscopy results showed that cobalt-manganese catalysts mainly composed of the spinel phase of Co_3O_4, Mn_2CoO_4 and/or$MnCo_2O_4$. The highest initial activity was presented bythe cobalt-manganese catalyst withahigh cobalt content.However, after 50-hours stability test the highest activity was presented by the cobalt-manganese catalyst with Co and Mn content close to the equimolar value.

1. INTRODUCTION

Since the 19th century it is observed a very intensive and continued development of technology and industry. Yet, still global energy demands is covered mainly by combustion of hydrocarbons that despite of carbon dioxide generates other environmentally harmful compounds, e.g., NO_X and products of incomplete combustion [1-2].

The use of technology based on catalytic combustion promotes reduction of emission of these additional pollutants. However, replacement of flame combustion of natural gas by catalytic flameless combustion is unlikely in the near future, inter alia due to the cost of remodelling combustion installations. Nevertheless, the technology based on catalytic combustion of hydrocarbons has many potential applications because it allows purification of air or other gas mixtures from very small amounts of combustible ingredients (hydrocarbons) at the same time generating energy gain. A common example given in this type of places is methane from the post-ventilation air of coal mines [3-5].

Palladium and platinum supported catalysts are the most frequently proposed systems for methane flameless combustion [6-11]. However, the high cost of catalysts based on noble metals is one of their main disadvantage. It is found that cobalt based materials demonstrate high catalytic activity in the oxidation process of hydrocarbons and volatile organic compounds [12-17]. However, cobalt-based catalysts suffer from lack of stability especially at high temperature. Some researchers prove that to overcome this problem it is required the use of a support material, for example: Al_2O_3 [13-15] or ZrO_2 [16-18].

Since, manganese oxides show better mechanical and thermal resistance in contrast to cobalt oxides and also demonstrate real catalytic activity in oxidation reactions [19] it is very interesting to prepare a physical mixture of cobalt and manganese-based materials. It is worth to mention that there are just a limited information in the literature [20-24] regarding the application of cobalt-manganese catalysts in the process of methane flameless combustion. Therefore, the subject of this research work is to fill this gap and compare catalytic systems based on cobalt and manganese oxides. Moreover, in the literature mentioned above, the results mainly focus on the course of light-off curves, which actually refer to initial activity of investigated catalytic materials.

2. MATERIALS AND METHODS

2.1. Catalytic systems preparation

Cobalt (Co) and manganese (Mn) catalysts were prepared by the precipitation method, while cobalt-manganese catalysts (0.8 Co–0.2 Mn and 0.6 Co–0.4 Mn) were obtained by the co-precipitation method with the use of acetates. The preparation was occurred in controlled conditions by applying the jacketed reactor form Radleys (U.K.). Water solution of ammonium carbonate was used as the precipitating agent and introduced to the reactor with the peristaltic pump at the constant rate of 5 cm^3/min, until pH = 8. After precipitation, the precipitate was filtered and washed with deionised water until pH reached 7. Next, the precipitate was washed with anhydrous alcohol and dried at room temperature by 12 hours. The last stage included drying at 383 K followed by calcination at 673 K by 2 hours.

2.2. Physicochemical characteristics

The content of metals was determined by X-ray fluorescence (XRF). The AxiosmAX spectrometer from PANalytical (The Netherlands) was applied. The analysis of results was carried out using the Omnian and Pro-Trace programs included in the SuperQ 5 software suite.

The basic information about the catalyst surface was obtained by the method of adsorption/desorption of nitrogen at the temperature of 77 K. Before the analysis a sample was degassed at 573 K. The test was carried out in the ASAP 2420 MP analytical system from Micromeritics Instrument Corporation (USA). It was assumed that the area occupied by one nitrogen atom is equal to 0.157 nm^2. The specific surface area was calculated based on the Brunauer-Emmett-Teller method [25-27], while the mean pore size and pore volume was determined using the Barret-Joyner-Halend method [28].

The bulk phase composition of studied catalytic systems was determined by X-ray diffraction (XRD). The high-resolution Empyrean X-ray diffractometer from PANalytical (The Netherlands) equipped with a lamp with a Cu anode was employed. The crystallographic phases present in the catalytic systems were identified based on the Joint Committee on Powder Diffraction

Standards (JCPDS) database. The quantitative fractions of individual phases were determined using Rietveld analysis [29-30].

The surface composition of obtained catalysts was analyzed using X-ray photoelectron spectroscopy (XPS). The multi-chamber UHV system from Prevac (Poland) equipped with a monochromatic Al Kα source MX-650 operating at 360 W and a hemispherical electron analyzer R4000 from VG Scienta (U.K.) was applied. The energy of the analyzer during the test was set at 200 eV (energy step – 0.5 eV) for survey scan and 50 eV (energy step – 0.1 eV) for the high resolution Co 2p and Mn 2p spectra.

2.3. Catalytic tests

The catalytic tests, i.e. studies of activity and stability of catalysts were conducted in the Microactivity Reference unit from PID Eng& Tech (Spain) equipped in the fixed-bed quartz reactor. The catalyst bed consisted of 50 mg of the catalyst sample mixed with 450 mg of quartz grains. The total volumetric flow rate of the reaction mixture, composed of 6 vol. % of methane, 18 vol. % of oxygen, 6 vol. % of argon and 70 vol. % of helium, through the catalytic bed was set to 100 cm^3/min.

The composition of the post-reaction mixture was analysed by an HPR 20 R&D quadruple mass spectrometer from Hiden Analytical (U.K.). During activity measures the temperature of the catalyst bed was linearly increased (5 K/min), while for stability tests the catalyst sample was maintained by 50-hours in isothermal conditions after reaching 773 K.

3. RESULTS AND DISCUSSION

3.1. Catalysts physicochemical properties

The XRF results (Table 1) show that the obtained catalysts contain various amounts of cobalt and manganese. The series of catalysts consist of four materials, two of them are reference, pure cobalt and manganese oxides and two mixed cobalt and manganese oxide materials at which Co:Mn molar ratio changes from 0.82:0.18 to 0.62:0.38.

Table 1. Metal content in the cobalt, cobalt-manganese and manganese catalysts determined by XRF

Catalyst	Metal content (wt. %)		Molar ratio (Co:Mn)
	Co	Mn	
Co	77.6	0	1:0
0.8 Co–0.2 Mn	60.9	12.8	0.82:0.18
0.6 Co–0.4 Mn	45.5	25.6	0.62:0.38
Mn	0	63.4	0:1

Table 2. Total BET surface area, average pore diameter and volume of pores determined for the cobalt, cobalt-manganese and manganese catalysts.

Catalyst	Total BET surface area (m^2/g)	Average pore diameter (nm)	Volume of pores (cm^3/g)
Co	29.1	20.95	0.138
0.8 Co–0.2 Mn	75.0	10.20	0.215
0.6 Co–0.4 Mn	82.4	8.83	0.218
Mn	58.1	10.58	0.186

The results of N_2 adsorption/desorption experiments (Table 2) show that cobalt-manganese catalysts have a higher total BET surface area than both manganese and cobalt catalysts. Moreover, their volume of pores is also much higher, while the average pore diameter is much lower than Co and Mn catalysts.

XRD results proved the crystalline structure of catalysts. Moreover, Rietveld refinement has successfully been applied to perform quantitative phase analysis and crystallite size calculation. Cobalt-manganese mixed oxide catalysts consist mainly of $MnCo_2O_4$ and Co_3O_4, while for higher amounts of manganese, Mn_2CoO_4 has also been identified (Table 3).

Table 3. Phases composition and mean size of crystallites determined on the base of XRD results for the cobalt, cobalt-manganese and manganese catalysts.

Catalyst	Crystallographic phases			Mean size of crystallites (nm)
	Chemical formula	Content (%)	Crystallite size (nm)	
Co	Co_3O_4	100	29.3	29.3
0.8 Co–0.2 Mn	Co_3O_4	98	10.8	10.8
	$MnCo_2O_4$	2	–	
0.6 Co–0.4 Mn	Co_3O_4	60	9.0	8.3
	$MnCo_2O_4$	26	5.0	
	Mn_2CoO_4	14	11.6	
Mn	Mn_2O_3	60	9.3	7.1
	Mn_3O_4	40	3.8	

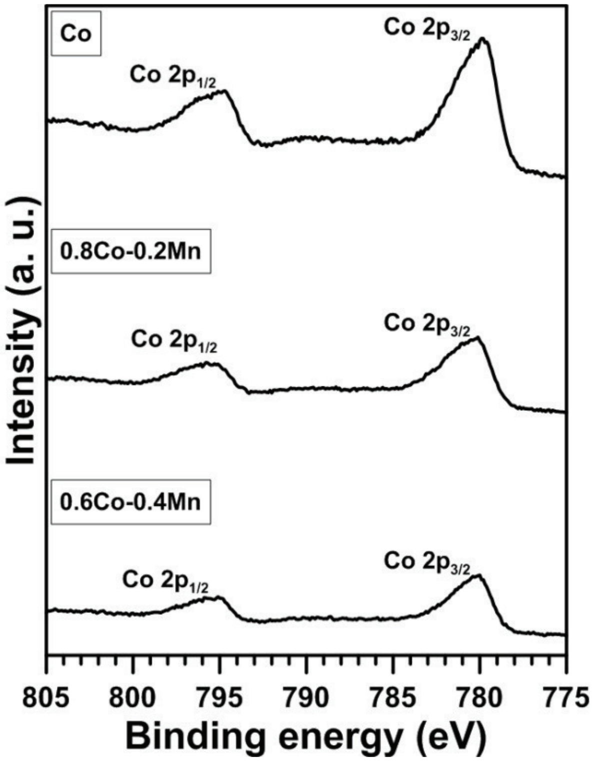

Fig. 1. The high resolution spectra of Co $2p_{1/2}$ and Co $2p_{3/2}$ for catalysts with cobalt.

For the pure oxides catalysts, both cobalt and manganese are presented in two oxidation states: +2 and +3. This results are also proved by XPS (Fig. 1 and 2) and are in line with some literature information [21].

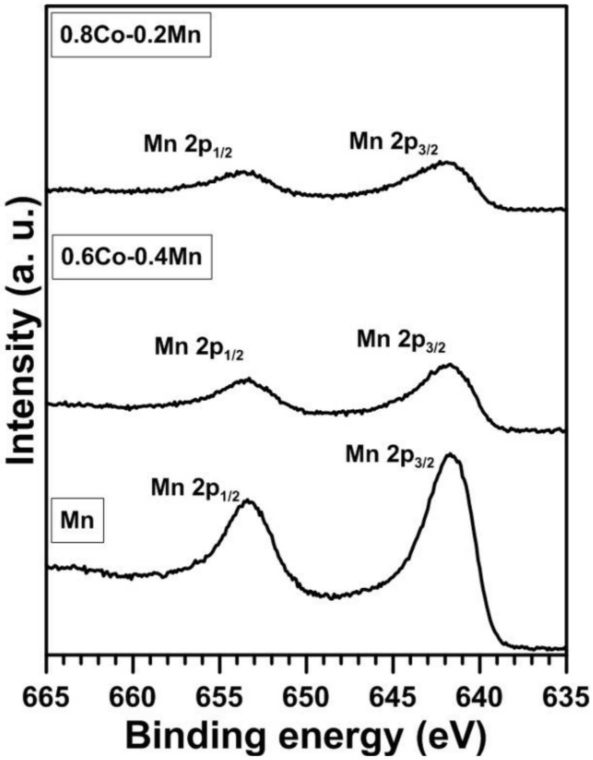

Fig. 2. The high resolution spectra of Mn $2p_{1/2}$ and Mn $2p_{3/2}$ for catalysts with manganese.

According to the crystallite size calculation the lowest mean size of crystallites is demonstrated by the manganese oxide catalyst and the greatest for the cobalt oxide catalyst. In fact the average size of crystallites for mixed cobalt and manganese oxides is located in the range between the values demonstrated for pure oxides catalysts and decreases together with the manganese content.

The results of the XPS analysis demonstrate that the surface of studied catalysts is composed of Co^{2+} and Co^{3+} (Fig. 1) and/or Mn^{2+} and Mn^{3+} (Fig. 2). The peak located at about 780 eV suggests the presence of the Co3O4 spinel phase, while the absence of the satellite peak at about 786 eV rather excludes the existence of the pure phase of CoO [24, 31, 32]. In the case of manganese, the peak located at about 642 eV suggests the presence of Mn^{3+} and probably spinel phase of Mn_3O_4, while the absence of the satellite peak at about 647 eV rather excludes an existence of the pure phase of MnO [24, 31, 33]. Moreover, the obtained results also rather do not indicate on the presence of Mn^{4+}.

3.2. Catalysts activity and stability

The light-off curves of methane flameless combustion are shown in Fig. 3. The results prove the highest activity for the pure cobalt and cobalt-manganese catalyst with a small amount of manganese. It was found that the addition of the larger amount of manganese causes a decrease in activity. The lowest activity is demonstrated by the pure manganese catalyst. The activity of these catalytic systems is comparable with activity of palladium catalysts with a small amount of palladium (< 0.4 wt. %). Moreover, these catalysts were more active than palladium-platinum and platinum catalysts tested earlier in our laboratory [34-36].

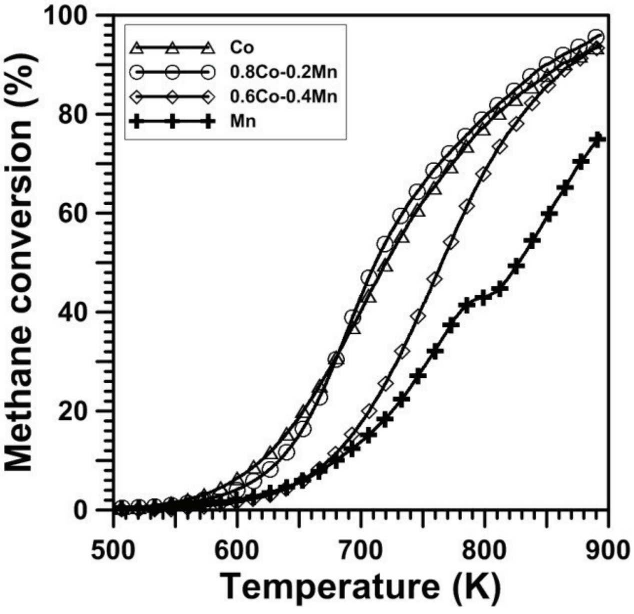

Fig. 3. The catalytic activity of the cobalt, cobalt-manganese and manganese catalysts for complete methane oxidation.

The one of the most important property of the catalyst it is the ability to maintain activity during the course of reaction. It is very important from the point of view of the practical application of the catalyst. It can be measured with the stability test shown in Fig. 4.

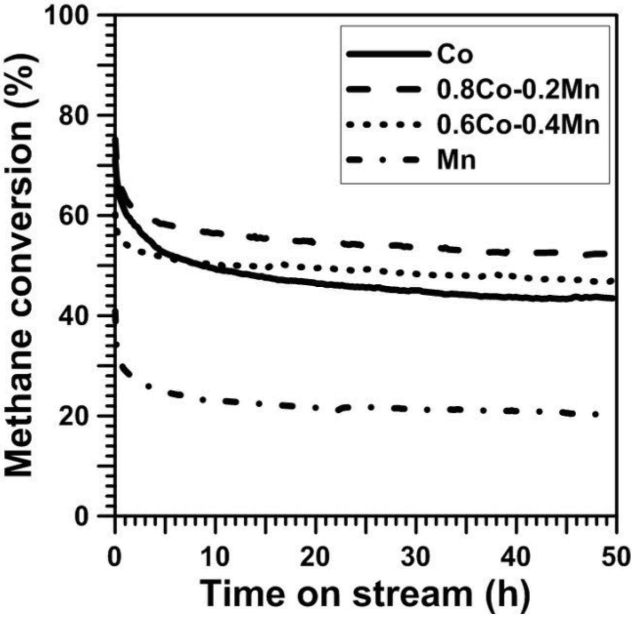

Fig. 4. The catalytic stability of the cobalt, cobalt-manganese and manganese catalysts in the process of complete methane oxidation

It is clearly visible that the activity of tested materials decreases during operation. After 50-hours conversion of methane dropped by 28 % for Co, by 23 % for 0.8Co-0.2Mn, by 14 % for 0.6Co-0.4Mn and by 19 % for Mn.

The obtained results show that the stability of the pure cobalt catalyst is the lowest, a little better is demonstrated by cobalt-manganese catalysts with the small amount of manganese, while the highest stability is shown for cobalt-manganese catalyst with the Co:Mn molar ratio equals 6:4.

Thus, present in the literature data [24], which suggest that the best catalytic properties towards methane combustion demonstrate cobalt-manganese catalysts with the small amount of manganese, are not entirely true. The light-off curves are providing only information about the initial activity. From the point of view of possibility of application of cobalt-manganese catalysts in the real industrial catalytic combustion of hydrocarbons, better properties are demonstrated by cobalt-manganese catalysts with the metal content (Co and Mn) close to the equimolar value than cobalt-manganese catalysts with a high predominance of cobalt.

CONCLUSIONS

The conducted research provided information about the activity and stability of cobalt-manganese catalysts mainly composed of the spinel phase of Co_3O_4, $MnCo_2O_4$ and/or Mn_2CoO_4. The obtained data suggest that cobalt-manganese catalysts with the metal content (Co and Mn) close to the equimolar value have better catalytic properties than cobalt-manganese catalysts with a high predominance of cobalt, and also are better compared to pure cobalt and manganese catalysts. Nonetheless, their properties are still far from ideal and probably before industrial application will require improvement, among others stability, e.g. use of highly resistive thermal and mechanical catalyst supports.

ACKNOWLEDGEMENTS

This research was funded by the National Science Centre as part of the Miniatura 1 project no. 2017/01/X/ST4/00334.

REFERENCES

[1] D. Ciuparu, M.R. Lyubovsky, E. Altman, L.D. Pfefferle, A. Datye, *Catalysis Reviews*, **44**, 593, (2002).

[2] C. Shao, W. Li, Q. Lin, Q. Huang, D. Pi, *Energy Technology*, **5**, 604, (2016).

[3] S. Su, J. Agnew,*Fuel*, **85**, 1201-1210, (2006).

[4] A. Setiawan, E.M. Kennedy, M. Stockenhuber, *Energy Technology*, **5**, 521-538, (2016).

[5] United States Environmental Protection Agency., https://www.epa.gov/sites/production/files/2019-11/documents/vam technologies. pdf, (2019).

[6] S. Ojala, N. Bion, A. Baylet, M. Tarighi, R.L. Keiski, D. Duprez, *Applied Catalysis B: Environmental*, **108**, 22, (2011).

[7] I. Friberg, N. Sadokhina, L. Olsson, *Applied Catalysis B: Environmental*, **231**, 242, (2018).

[8] N. Sadokhina, G. Smedler, U. Nylén, M. Olofsson, L. Olsson, *Applied Catalysis B: Environmental*, **236**, 384, (2018).

[9] X. Zhao, Y. Liu, J. Deng, P. Xu, J. Yang, K. Zhang, Z. Han, H. Dai, *Molecular Catalysis*, **442**, 191, (2017).

[10] L. Urfels, G. Gélin, M. Primet, E. Tena, *Topics in Catalysis*, **30**, 427, (2004).

[11] A. Gremminger, P. Lott, M. Merts, M. Casapu, J-D. Grunwaldt, O. Deutschmann, *Applied Catalysis B: Environmental*, **218**, 833, (2017).

[12] Z. Chen, S. Wang, W. Liu, X. Gao, D. Gao, M. Wang, S. Wang, *Applied Catalysis A: General*, **525**, 94, (2016).

[13] U. Zavyalova, P. Scholz, B. Ondruschka, *Applied Catalysis A: General*, **323**, 226, (2007).

[14] Q. Wang, Y. Peng, J. Fu, G.Z. Kyzas, S.M. Reduwan-Billah, S. An, *Applied Catalysis B: Environmental*, **168-169**, 42, (2015).

[15] P. Stefanov, S. Todorova, A. Naydenov, B. Tzaneva, H. Kolev, G. Atanasova, D. Stoyanova, Y. Karakirova, K. Aleksieva, *Chemical Engineering Journal*, **266**, 329, (2015).

[16] L.F. Liotta, G. Di Carlo, G. Pantaleo, G. Deganelleo, *Catalysis Communications*, **6**, 329, (2005).

[17] J.P. Jodłowski, J.R. Jędrzejczyk, K.D.Chlebda, A.Dziedzicka, Ł. Kuterasiński, A. Gancarczyk, M. Sitarz, *Nanomaterials*, **7**,174, (2017).

[18] D. L. Ileana, A. Carrascull, M. Ponzi, E.N. Ponzi, I. L. Botto, *Materials Chemistry and Physics*, **92**, 327, (2005).

[19] S. Ordóñez, J.R. Paredes, F.V. Díez, *Applied Catalysis A: General*, **341**, 174, (2008).

[20] X. Wang, Y. Xie, *Reaction Kinetics and Catalysis Letters*, **70**, 43, (2000).

[21] W. Li, Y. Lin, Y. Zhang, *Catalysis Today*, **83**, 239, (2003).

[22] M. Kumar, G. Rattan, *Journal of Chemical Technology and Metallurgy*, **51**, 63, (2016).

[23] A. N. Zabidi Mohd, R. Pilus, S. Rahman, S. Ali, *Material research innovation*, **18**, 477, (2014).

[24] J. Li, X. Liang, S. Xu, J. Hao, *Applied Catalysis B: Environmental*, **90**, 307, (2009).

[25] S. Brunauer, P.H. Emmett, E. Teller, *Journal of the American Chemical Society*, **60**, 309, (1938).

[26] M. S. Mel'gunov, A. B. Ayupov, *Microporous and Mesoporous Materials*, **243**, 147, (2017).

[27] M. Thommes, K. Kaneko, V. A. Neimark, P. J. Olivier, F.Rodriguez-Reinoso, J. Rouquerol, S. W. K. Sing, *Pure and Applied Chemistry*, **87**, 1051, (2015).

[28] L. G. Joyner, E. P. Barrett, R. Skold, *Journal of the American Chemical Society*, **73**, 3155, (1951).

[29] H. M. Rietveld, *Journal of Applied Crystallography*, **2**, 65, (1969).

[30] G.A. Calliraris, T.L.T. Da Silva, A.P.B.Ribeiro, A.O.Dos Santos, L.P. Cardoso, *Chemistry and physics of lipids*, **212**, 51, (2018).

[31] M. C. Biesinger, B. P. Payne, A.P. Grosvenor, L. W. M. Lau, A. R. Gerson, R. S. C. Smart, *Applied Surface Science*, **257**, 2717, (2011).

[32] M. Greluk, M. Rotko, G. Słowik, S. Turczyniak-Surdacka, *Journal of the Energy Institute*, **92**, 222, (2019).

[33] K. Ramesh, L. Chen, F. Chen, Y. Liu, Z. Wang, Y. F. Han, *Catalysis Today*, **131**, 477, (2008).

[34] A. Machocki, M. Rotko, W. Gac, *Topics in Catalysis*, **52**, 1085, (2009).

[35] M. Rotko, A. Machocki, G. Słowik, *Catalysis Letters*, **147**, 1783, (2017).

[36] M. Rotko, A. Machocki, G. Słowik, *Applied Catalysis B: Environmental*, **160-161**, 298, (2014).